rhd instruments
flexible cell solutions

Application note

Electrochemical corrosion studies of various metals

- 1.4301 stainless steel
- Nickel thin film
- S235 steel

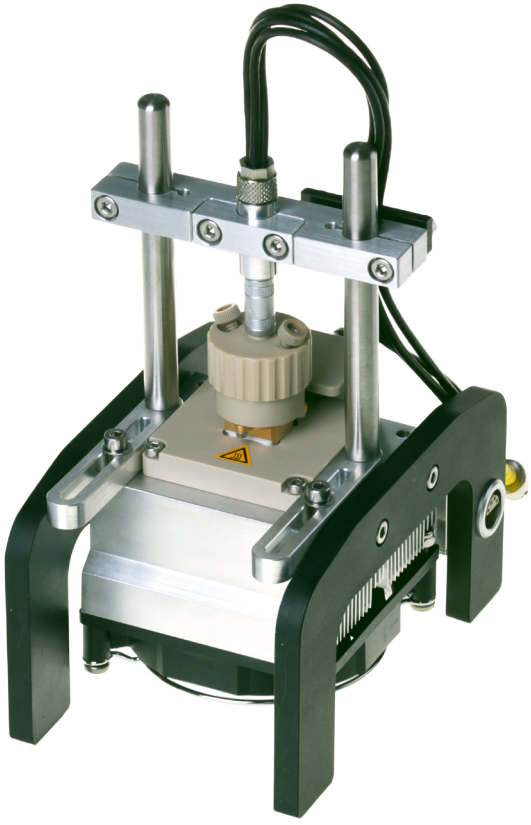

Mareike Länger

Introduction

Corrosion is the degradation of a material's mass or properties over time caused by environmental effects [1]. Metallic corrosion is a problem seriously affecting not only many industrial sectors, but also private life resulting in enormous costs [2]. According to government and industry studies, over $220 billion is lost to corrosion in the United States each year [2]. In consequence, corrosion protection is a large research field and many different approaches exist depending on the desired application and environmental requirements. Common methods are for example the application of paint films on metals preventing in the simplest case its direct contact with the corrosive medium, usage of inhibitors which e.g. scavenging the corrosive substances in the medium or cathodic protection, i.e. the usage of potential differences to force the corrosion to occur on a sacrificial anode [2].

Various types of corrosion exist, being classified based on morphology or mechanism [2]. Subdivisions are for example uniform, crevice, pitting or localized corrosion, environmentally assisted or stress corrosion cracking and galvanic corrosion [2]. Galvanic corrosion, typically resulting in a rather rapid attack, occurs if a less noble metal is in electrical contact with a more noble one in an electrolyte [2]. Electrical generated externally currents like stray ground currents from large electrical equipment could be an additional source of potential differences resulting in galvanic corrosion [2].

Due to the numerous types of corrosion occurring on different materials in various environments like steel in concrete, aluminium pipes, corrosion of ship components in seawater or even titanium and titanium alloys in surgical implants and nickel-chromium alloys in dental inlays, numerous publications dealing with a specified problem using a test method adapted to the distinct environmental requirements exist [2], [3], [4]. In consequence, the results are hardly comparable and only few general measurement norms exist [5]. In this application note, we nevertheless tried to compare the results we gained during electrochemical corrosion studies on different metals to literature data. Unfortunately, in literature no corrosion rates for the different metals using the same testing method could be found. Therefore, the experiments presented in the following vary from one metal to the other to reproduce the test methods reported in literature for the respective metal as good as possible. This is even more complicated as the exact metal composition under investigation and its history like surface treatment during fabrication is often not exactly described, but influences the resulting corrosion rate [6].

In corrosion science often the question about the timing of some corrosion events arises like how long before corrosion will result in a leak or vessel rupture [2]. Thus, knowledge of corrosion rates is of high interest. Unfortunately, they tend to vary notoriously [2]. Thus, in some cases precise predictions proved to be impossible. Nevertheless, if their limitations are understood, they can be really useful and corrosion rates have been published for numerous material combinations and environments [2]. Typically, these rates are averages over many tests as the result of a single sample may deviate distinctly from the mean, but in aggregate reliable values can be achieved [2]. Usually, corrosion rates are given as mass loss per unit area and unit time or by means of the thickness loss as rate of penetration and expressed either as mpy (milliinches per year) or mmpy (millimeter per year) [4].

[1] ***Corrosion Engineering Handbook***, P.A. Schweitzer (Ed.), 1996, Marcel Dekker, Inc.

[2] ***Uhling's Corrosion Handbook, 3rd Edition***, R. Winston Revie (Ed.), 2011, John Wiley & Sons, Inc.

[3] M. Pourbaix, ***Biomaterials*** **5**, 3 (1984), 122-134

[4] A. Cinitha et al., ***KSCE Journal of Civil Engineering*** **18**, 6 (2014), 1735-1744

[5] e.g. ASTM standards G5, G59, G61, G102

[6] M. Warzee et al., ***J. Electrochem. Soc.*** **112**, 7 (1965), 670-674

The damage caused by corrosion is evaluated either by studying mass or thickness losses with time or by electrochemical methods [4]. While the first method often requires larger test specimen and longer times, the second one is more suitable for laboratory use.

Corrosion rates of less than 3 mpy are acceptable for most chemical processes and structures, materials showing rates between 2 and 20 (partially 50) mpy are considered useful for the given environment, while those exhibiting higher rates are usually unacceptable [1].

Short summary of corrosion theory

The oxidation of a metal exposed to a strong acid is one of the most basic corrosion reactions. E.g. pure iron in hydrochloric acid results in the gradual disappearance of the iron specimen and the formation of hydrogen bubbles [1]:

$$Fe(s) + 2HCl(aq) \rightarrow Fe^{2+}(aq) + 2\,Cl^{-}(aq) + H_2(g)\uparrow$$ **(Equation 1)**

Thereby, an iron atom is oxidized to an iron ion by releasing two electrons. These are taken from the hydrogen ions being thus reduced and form hydrogen gas. The electron transfer occurs at the metal surface [1]. The faster the dissolution of the metal, the higher the current flow. The overall corrosion reaction can be divided in the cathode and anode half cell reaction [1]:

$$2H^{+}(aq) + 2e^{-} \rightarrow H_2(g)\uparrow \qquad \text{(Equation 2)}$$
$$Fe(s) \rightarrow Fe^{2+}(aq) + 2e^{-}$$

The standard redox potential of the respective reactions is tabulated and for deviations from the standard conditions, they can be calculated using the Nernst equation [1], [7]. The larger the difference between potentials of the anodic and cathodic half cell reaction, the higher the driving force for the reaction [1]. In a closed electrochemical circuit current begins to flow and the potentials of both half cell reactions move toward each other [1]. The point at which the currents are equal defines the corrosion potential E_{corr} and the resulting current is the so called corrosion current i_{corr}[1].

a) *Butler-Volmer formalism for a half cell reaction*

In case a current passes through an electrochemical cell, the half cell potentials shift from their equilibrium values with the deviation labeled overpotential or overvoltage η [7]:

$$\eta = E(i) - E_0 \qquad \textbf{(Equation 3)}$$

where E_0 is the half cell equilibrium potential and $E(i)$ is the potential represented as function of current density i [7].

In electrochemical systems where the reaction rate is determined by the charge transfer at the metal surface as it holds for corrosion measurements at least in the vicinity of the corrosion potential the current-voltage relation can be described by the Butler-Volmer equation [7], [8]:

$$i = i_a + i_c = i_0 \left\{ \exp\left[\frac{\alpha n F}{RT} \eta \right] - \exp\left[-\frac{(1-\alpha) n F}{RT} \eta \right] \right\}$$ **(Equation 4)**

where i, i_a and i_c are the current densities of the complete reaction and the anodic and cathodic branch, respectively, i_0 is the exchange current density, α is the so called transfer coefficient, n is the number of transferred electrons, F is the Faraday constant, R *is* the gas constant and T is the temperature [8]. In case $|\eta|$ is distinctly larger than $\frac{RT}{nF}$ $\left(= \frac{25.7}{n}\ \text{mV}\right.$ at 25 °C) the respective counter-reaction can be neglected, leading for the cathodic branch to:

$$i = -i_0 \exp\left[-\frac{(1-\alpha) n F}{RT} \eta \right] \qquad \textbf{(Equation 5)}$$

After logarithmising and rearranging η can be expressed as:

$$\eta = \frac{RT}{(1-\alpha)nF} 2.3 \lg i_0 - \frac{RT}{(1-\alpha)nF} 2.3 \lg |i| \qquad \textbf{(Equation 6)}$$

[7] ***Fundamentals of Electrochemical Corrosion***, E. E. Stansbury, R. A. Buchanan, 2000, ASM International

[8] ***Elektrochemie***, C. H. Hamann, W. Vielstich, 3. völlig überarbeitete und erweiterte Auflage 1998, Wiley-VCH

thus yielding the form of a linear equation $\eta = A + B \cdot \lg|i|$; this type of notation is known as Tafel form [8]. Please note that lg is the logarithm to the basis 10.

The same holds for the anodic branch:

$$i = i_0 \exp\left[\frac{\alpha n F}{RT}\eta\right]$$

$$\eta = -\frac{RT}{\alpha n F}2.3\lg i_0 + \frac{RT}{\alpha n F}2.3\lg|i| \qquad \textbf{(Equation 7)}$$

Constant B is named Tafel constant being defined for the anodic (B_a) and cathodic (B_c) branch, respectively, as

$$B_a = \frac{2.3RT}{\alpha n F} \qquad B_c = \frac{2.3RT}{(1-\alpha)nF} \qquad \textbf{(Equation 8)}$$

b) *Corrosion analysis*

As discussed above if the two half cell reactions are in equilibrium a mixed potential, i.e. E_{corr}, adjusts. Deviations from equilibrium are e.g. induced by applying an external positive or negative polarization potential E_{ext} to the system. Small deviations are associated with charge transfer polarization with the overpotential η_{CT} designated as [7]

$$\eta_{CT} = E_{ext} - E_{corr} \qquad \textbf{(Equation 9)}$$

During corrosion analysis, it is assumed that over the potential range of interest the contribution of the currents of the respective reverse reactions, i.e. in the example presented above the reduction of iron and the oxidation of hydrogen, are negligible [7]. Thus, the equations for the oxidation and reduction current densities i_{ox} and i_{red}, respectively, reduce to [7], [9]*:

$$i_{ox} = i_{corr}\exp\left[\frac{2.3}{B_{a,M}}\eta_{cT}\right] \quad |i_{red}| = i_{corr}\exp\left[-\frac{2.3}{B_{c,X}}\eta_{CT}\right] \qquad \textbf{(Equation 10)}$$

Thereby, $B_{a,M}$ and $B_{c,X}$ symbol the Tafel constants of the metal oxidation branch and the reduction branch of the species to be reduced, i.e. in the example above hydrogen. Please note that in corrosion science close to E_{corr} the exchange current density is labeled corrosion current density i_{corr}; this convention will be complied in the subsequent manuscript.

The measured current density i_{net} is the difference of the oxidation and reduction current density:

$$i_{meas} = i_{ox} - |i_{red}| = i_{corr}\left\{\exp\left[\frac{2.3}{B_{a,M}}\eta_{CT}\right] - \exp\left[-\frac{2.3}{B_{c,X}}\eta_{CT}\right]\right\} \qquad \textbf{(Equation 11)}$$

As can be seen from this equation, if η_{CT} approaches zero, $|i_{meas}|$ also approaches zero as the current resulting from the oxidation reaction equals that of the reduction reaction. Thus, the net flow is zero and the curves become asymptotic to the equilibrium potential, i.e. E_{corr}, see Figure 1 plotting $|i_{meas}|$ in logarithmic scale as function of η_{CT} [7]. At this point a state of dynamic equilibrium exists and i_{ox} as well as i_{red} are equal to the exchange current density and thus the corrosion current density [7]. It can be determined by extrapolation of the respective Tafel equation to the linear portion of the cathodic and anodic branch of the measured current [7]: At sufficient large positive or negative overpotentials Equation 11 reduces to the equation of a single oxidation or reduction reaction, respectively, as the respective other exponential becomes negligible and the branches become linear, thus corresponding to the respective Tafel equation [7]. This equation would plot exactly like the respective linear portion in Equation 11 but would extend as shown by the dashed portion of the line in Figure 1. The intersection of both extrapolations delivers the corrosion potential as well as the corrosion current. If only one branch shows sufficient linear portion - in most cases the cathodic branch - the intersection of the dashed extension with the ordinate value corresponding to E_{corr} is the corrosion current [7]. For many metals and alloys the anodic branch does not show sufficient linear portion due to active-passive behaviour [7]. In case the corrosion is under diffusion control

[9] ***Lehrbuch der Physikalischen Chemie***, G. Wedler, Fünfte vollständig überarbeitete und aktualisierte Auflage 2004, Wiley-VCH

* By definition, the cathodic current is set negative. Thus, for the resulting current density holds: $i = i_a + i_c = i_a - |i_c|$ [7], [9]

or the nature of the interface changes with changing potential a linear region may be also not observed in the cathodic branch [7].

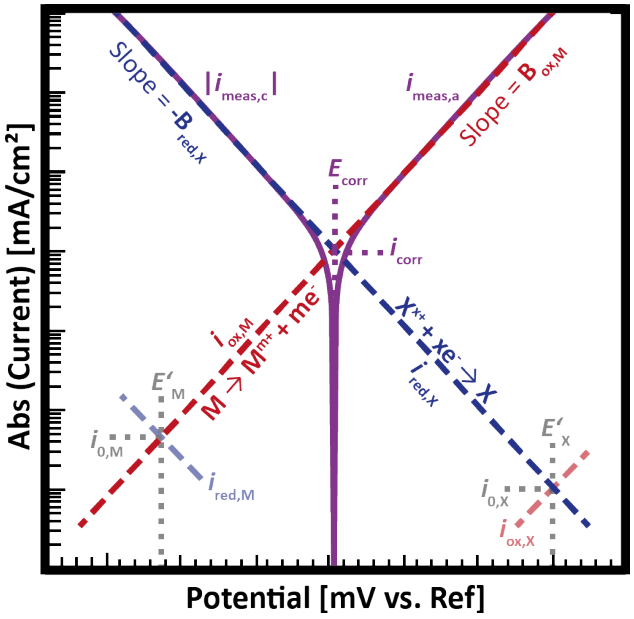

Figure 1: Schematic experimental polarization curves (violet) plotting the logarithm of the absolute value of the measured current density assuming Tafel behaviour for the individual oxidation (red) and reduction (blue) reaction polarization curves. Slopes of the individual linear regions correspond to the respective Tafel constant. M, M^{m+}, X^{x+} and X symbol the oxidized and reduced form of metal and the species being reduced during corrosion experiments (e.g. hydrogen), respectively, E'_M and E'_X the respective equilibrium half cell potential, $i_{0,M}$ and $i_{0,X}$ the respective exchange current density, $i_{red,M}$ and $i_{red,X}$, $i_{ox,M}$ and $i_{ox,X}$ the respective reduction and oxidation current density of the two half cell reactions (given for the example above in Equation 2). Modified and redrawn from [7].

Assuming equal values for both the transfer coefficient of the metal oxidation $\alpha_{a,m}$ and that of the reduction of the species to be reduced $\alpha_{c,X}$, i.e. $\alpha = \alpha_{a,m} = \alpha_{c,X}$, in case of small overvoltages of less than 10 mV the exponents are small enough that the series expansion of Equation 10 can be truncated after the second term ($e^x = 1 + x$ for small x) resulting in the following expression for the Butler-Volmer equation [8]:

$$i = i_{corr}\left\{1+\frac{\alpha nF}{RT}\eta_{CT}-\left[1-(1-\alpha)\frac{nF}{RT}\eta_{CT}\right]\right\} = i_{corr}\frac{nF}{RT}\eta_{CT}$$

(Equation 12)

Thus, for $|\eta_{CT}| \leq 10$ mV the current-overpotential curves become linear with a slope only dependent on i_{corr} but not on α [8]. The term $\frac{RT}{nFi_{corr}} = \frac{d\eta}{di}$, i.e. the slope of the line, has units of resistance, thus being labeled polarization resistance R_p*. It can be used for determination of i_{corr} [2]. Please note, that this is only a rough assumption as for real samples the α values could differ from each other significantly. In this case, values for the Tafel constants either determined from experiments or taken from literature have to be used for calculation of i_{corr}, see the footnote at the bottom of this page.

After determination of the corrosion current density the corrosion rate can be calculated using Faraday's law with n as number of transferred electrons, W as weight of the electroactive species, i.e. the mass of the species that has reacted, F as Faraday constant, M as atomic weight and t as time [7]:

$$i_{corr} = \frac{nWF}{Mt} \qquad \textbf{(Equation 13)}$$

M/n is the so called equivalent weight defined as the atomic weight of the element divided by the number of electrons required to oxidize an atom of the element in the corrosion process, that is, the valence of the element [5].

Solving Equation 13 for W/t and division by density ρ of the material results in the corrosion penetration rate CPR in cm/s:

$$CPR = \frac{Mi_{corr}}{nF\rho} \qquad \textbf{(Equation 14)}$$

* R_p can also be expressed using Tafel constants B_a and B_c:

$$\frac{d\eta}{di} = \frac{B_{a,M}\cdot B_{c,X}}{2.3i_{corr}\cdot\left(B_{a,M}+B_{c,X}\right)} = R_p \quad \text{(Equation 12.1)}$$

This equation is derived from Equation 12 by insertion the expressions for Tafel constants B_a and B_c:

$$i = i_{corr}\left\{1+\frac{2.3}{B_{a,M}}\eta_{CT}-\left[1-\frac{2.3}{B_{c,X}}\eta_{CT}\right]\right\} = 2.3i_0\frac{B_{a,M}+B_{c,X}}{B_{a,M}\cdot B_{c,X}}\eta_{CT} \quad \text{(Equation 12.2)}$$

Solving this expression for i_{corr} leads to

$$i_{corr} = \frac{B_{a,M}\cdot B_{c,X}}{2.3R_p\cdot\left(B_{a,M}+B_{c,X}\right)} \quad \text{(Equation 12.3)}$$

which is often used in corrosion science in case the Tafel slopes are known for the reaction under investigation for calculation of the i_{corr} from the corrosion resistance.

More commonly, CPR is expressed as mmpy (mm per year) or mpy (milliinches per year) [7]:

$$CPR(mmpy) = C_{mmpy} \frac{Mi_{corr}}{n\rho}$$
$$CPR(mpy) = C_{mpy} \frac{Mi_{corr}}{n\rho} \qquad \textbf{(Equation 15)}$$

with $C_{mmpy} = 3.27 \cdot 10^{-3}$ mm·mol/(µA·cm·y) and $C_{mpy} = 0.129$ mi·mol/(µA·cm·y), respectively, y as year and mi as milliinch; i_{corr} is given in units of µA/cm², otherwise the constants need to be adapted.

Electrochemical methods for corrosion studies

There are several electrochemical methods for studying corrosion phenomena and determination of corrosion rates [2], [7]. In the following, four well established procedures will be shortly presented. For more detailed insight, the reader is referred to literature, see for example [2], [7].

a) *Polarization resistance technique*

A very well established method for both corrosion prediction and monitoring is the linear polarization or polarization resistance technique [2]. It is not only rapid, simple, and relatively inexpensive, but moreover can be applied without detailed knowledge of the controlling electrochemical parameters in complex, poorly defined electrolytes [2]. Using this method, the realistic limit for corrosion rate estimation is about 0.001 mm/year (0.1 mpy) mostly because of limitations in estimating Tafel slopes [2]. ASTM standard G59 describes the general test procedure. In this method, the specimen is stored for 55 min in the test solution for determination of the open circuit corrosion potential [7]. Thereafter, a potentiodynamic polarization curve is recorded starting 30 mV more negative and ending 30 mV more positive than the corrosion potential [5]. The polarization resistance is the reciprocal of the slope of the polarization curve at the corrosion potential when plotted with voltage and current density on the abscissa and ordinate, respectively [2]. As long as the polarization is in the vicinity of the corrosion potential, i.e. ~± 30 mV or less, the measurement does not interfere with the quantities being measured [2]. In consequence, as the material surface is expected to remain unchanged, repeated measurements can be performed without re-preparing the sample [7]. For calculation of the corrosion current, see the definition of R_P, $\frac{RT}{nFi_{corr}} = \frac{d\eta}{di}$, or Equation 12.3, (partly) the two Tafel constants, i.e. the slopes of the anodic and cathodic branch of the measured curve, and the polarization resistance, all measured at the corrosion potential, are required [2]. Their determination usually requires regression analysis [2].

b) *Electrochemical impedance spectroscopy*

Electrochemical impedance spectroscopy is also a routine tool for practical corrosion prediction [2]. It enables a rapid estimation of corrosion rates lower than 10^{-4} mm/year and can be applied even in low-conductivity media [2]. Using a suitable equivalent circuit the corrosion resistance can be determined. Using the definition of R_P or Equation 12.3, it can be used for calculation of the corrosion current density. Thus, partly knowledge of the Tafel constants for the given material system might be required [7]. If they are unavailable or not easily obtained, a value of 0.025 V can be used for Tafel constant B ($= \frac{B_a \cdot B_c}{2.3(B_a + B_c)}$), likewise assuming equal values for both transfer coefficients $\alpha_{a,m}$ and $\alpha_{c,X}$ [2], [5]. However, this might result in errors greater than 50 % [2].

c) *Potentiodynamic polarization technique*

Like the linear polarization resistance method the (cyclic or anodic) potentiodynamic polarization technique continuously ramps the applied potential usually starting at the corrosion potential in direction of more positive potential [2]. Partially, the voltage is reversed

at some chosen potential and scanned in cathodic or active direction to the corrosion potential or a potential active with respect to it [2]. ASTM standard G61 describes the general test procedure. This technique is used for prediction of localized corrosion, but should not be used to determine the uniform rate of corrosion as the latter case would require the assumption that the corrosion mechanism does not change over a potential range of several hundred millivolts which may not be valid [2]. Potentiodynamic polarization curves are interpreted using the relationship between current and voltage as well as differences between forward and reverse scan thus delivering information e.g. about the repassivation or protection potential and the pitting potential [2]. However, as main focus of this application note is the determination of corrosion rates, details about these features and their determination from measurement data is beyond the scope of this report. A detailed discussion dealing with these features as well as limitations and pitfalls of all electrochemical techniques presented here can be found in literature, see for example [2].

d) *Tafel extrapolation*

Yet another technique for determination of uniform corrosion rates is the Tafel extrapolation [7]. In this technique, the applied potential is likewise continuously ramped, but over a medium potential range of usually ± 300 mV vs. the corrosion potential [7]. Such a broad range greater than ± 50 to 100 mV compared to E_{corr} is required to reach potentials at which either the anodic or cathodic reaction dominates (i.e. $25.7/n$ mV to guarantee for reaching the linear region and some range to actually perform the linear extrapolation) [7]. However, as result of such large deviations from E_{corr} conditions at the metal/solution interface may change progressively, including IR potential drops between working and reference electrode or diffusion of species from and to the interface, and prevent linear behaviour [7]. For reliable Tafel extrapolation linear section of at least one decade of current is required [7].

In general during corrosion analysis invoking the assumption of linearity for determination of Tafel slopes where the curve is actually nonlinear has been estimated to cause errors as high as 50 % [2]. However, this may be acceptable as corrosion rates estimated from mass loss can result in errors of 100 % [2]. In consequence, during screening, rates differing by a factor of 2 or 3 may be considered to be the same [2].

Experimental

For electrochemical determination of the corrosion rate of the diverse metal specimen a TSC surface measuring cell, see Figure 2, in combination with a Microcell HC setup has been used. This measuring cell enables e.g. the electrochemical characterization of solid/liquid interfaces and surface characterization of planar, moisture-, air- or photosensitive substrates of variable shape under temperature control. The PEEK casing guarantees hermetic sealing of the cell interior from the outside. The o-ring pressed from above onto the surface of the sample restricts the active surface to 0.283 cm^2.

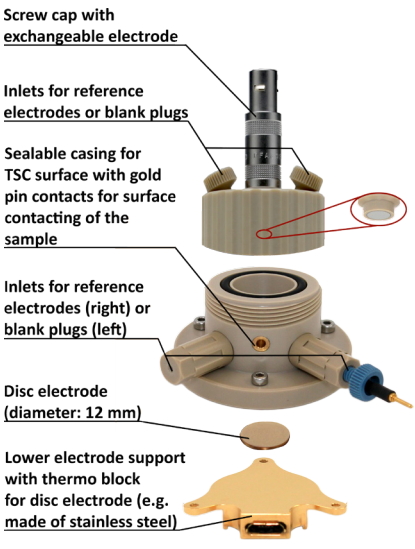

Figure 2: Exploded view of measuring cell TSC surface. The solid sample is placed on the lower electrode. Its active surface is restricted by an o-ring being pressed from above onto it. For surface studies of the solid sample the gold pin contacts are used for contacting. The liquid electrolyte is inserted from above. The two plugs laterally screwed into the casing enable the insertion of reference electrodes.

The inlets in the cap also enable the employment of reference electrodes or can be used as gas inlet/outlet.

Besides measuring cell TSC surface mounted onto the Microcell HC setup, a Metrohm Autolab PGSTAT204 equipped with a FRA32-module was used for the electrochemical analysis. For data acquisition, the NOVA 1.11 software (Metrohm Autolab B.V.) has been employed. In the Microcell HC setup, temperature is controlled via a Peltier element which enables adjusting sample temperatures ranging from -40 °C up to +100 °C, depending on dew point and sample amount. In combination with a Microcell HC setup the temperature accuracy is 0.1 °C in the thermo block.

Composition of the diverse metal specimen as specified for the respective alloy is given in Table 1. Nickel thin films (TF) were electrochemically deposited onto polished stainless steel substrates.

Table 1: Composition and fabrication details of the metal specimen characterized in this application note.

Alloy	Composition [%]	Fabrication remarks
Stainless steel 1.4301	$C \leq 0.07$ $P \leq 0.05$ $Mn \leq 2.00$ $Si \leq 1.00$ Cr 17.5 - 19.5 $S \leq 0.03$ Ni 8.00 - 10.5 $N \leq 0.11$ Fe Balance	(a) turned of stainless steel rod (b) laser cut from rolled stainless steel sheet, polished down to grain size of 1 µm (c) laser cut from rolled stainless steel sheet, abrasive paper of grid size 1200
Nickel thin film	pure nickel	electrochemical deposition at 40 °C on polished stainless steel; either 3 min at 3 V or 6 min at 2 V
Steel S235	$C \leq 0.22$ $Cr \leq 0.3$ $Mn \leq 1.6$ $Si \leq 0.05$ $P \leq 0.05$ $S \leq 0.05$ $Cu \leq 0.3$ $N \leq 0.012$ Fe Balance	-

In case of stainless steel 1.4301 three differently treated sets of specimen were studied to investigate the influence of the surface treatment on the corrosion rate. While one set of specimen was turned of a stainless steel rod (a) the other two sets were laser cut from a rolled stainless steel sheet. One was polished using diamond paste down to a grain size of 1 µm (b) and the other one was treated using abrasive paper grid size 1200 with ethylene glycol (c).

Experimental procedures for the different metal specimen were adopted from the respective literature and are summarized in Table 2. Only the potential windows were reduced as at potentials far away from the corrosion potential distinct gas formation (presumably H_2) going along with bubble formation occurs leading to partial contact loss. During selection of the potential windows care was taken that they are sufficient wide for proper Tafel evaluation. pH of the electrolyte used for corrosion study of the nickel thin films was adjusted using dilute sulfuric acid.

Table 2: Experimental procedures for the different metal specimen together with the respective literature specified in the square brackets. Potentials were recorded vs. Ag/AgCl (3 mol/l KCl) reference.

Alloy Literature	Electrolyte	Potential range [V]	Scan rate [mV/s]	Temperature [°C]
Stainless steel 1.4301 [10]	2 mol/l HCl	-0.45 to -0.17*	1.66	20.0
Nickel TF [11]	0.5 mol/l Na_2SO_4 (pH ~ 2)	-0.55 to +0.15	1.00	25.0
Steel S235 [12]	0.5 mol/l HCl	-0.70 to -0.40	0.50	25.0

In each case, the respective specimen and a polished platinum electrode, 6 mm in diameter, were used as working and counter electrode, respectively. As reference electrode a Ag/AgCl electrode (+210 mV/NHE, checked vs. commercial Ag/AgCl reference) made of a silver wire coated with AgCl in 3 mol/l KCl solution and in contact with the cell compart-

[10] R. T. Loto et al., ***J. Mater. Environ. Sci.*** **6**, 9 (2015) 2409-2417

[11] D. E. Rusu et al., ***J. Coat. Technol. Res.*** **9**, 1 (2012) 87-95

[12] D. Gassama et al., ***Bull. Chem. Soc. Ethiop.*** **29**, 2 (2015) 299-310

[13] C. Kuphasuk et al., ***J. Prosthetic Dentistry*** **85**, 2 (2001), 195-202

* For one single measurement of the polished specimen the upper potential limit was set to -0.25 V, linear Tafel analysis was nevertheless possible.

ment via a ceramic frit was used. Approximately 0.9 ml of the respective electrolyte was inserted into the measuring cell.

Electrochemical studies were performed at the respective temperatures given in Table 2. Normally, a measurement was started directly after assembling of the measuring cell and short determination of the open circuit potential. Before the polarization experiment depending on the corrosive behaviour of the sample-electrolyte combination an impedance spectrum was recorded at open circuit potential in 3-electrode configuration for frequencies ranging from 500 kHz down to 10 Hz while applying an ac-voltage amplitude of 10 mV (rms) to the sample. If the sample-electrolyte combination was too corrosive so that corrosion going along with distinct bubble formation took already place during impedance measurement, the latter measurement was set aside. Linearity was proofed for the frequency range of interest using Kramers-Kronig Test [14]. For fitting of the impedance data the impedance analysis software RelaxIS® distributed by rhd instruments GmbH & Co. KG was used.

Results and discussion

For each different metal specimen at least three measurements were performed as common in literature [12], [13]. For Tafel evaluation the measured current density was plotted on logarithmic scale vs. the applied potential and slopes of the cathodic and anodic branch were determined via linear extrapolation of the respective linear region of the curve. Corrosion rates were calculated using equivalent weights tabulated in ASTM standard G102. The resulting mean values for the corrosion rate, the corrosion current as well as the corrosion potential are summarized in Table 3 together with the values reported in literature. Exemplary polarization curves for each of the diverse metal specimen are presented in Figures 3 to 5.

Table 3: Mean values for the corrosion rate, the corrosion current density as well as the corrosion potential for the different metal specimen. Errors are given as maximal deviation from the mean. The respective literature values are given in brackets. Potentials were recorded vs. Ag/AgCl (3 mol/l KCl) reference. Different treatment of the stainless steel (SS) specimen: (a) turned of stainless steel rod; (b) laser cut from rolled stainless steel sheet, polished; (c) laser cut from rolled stainless steel sheet, abrasive paper.

Alloy	E_{corr} [V]	Error E_{corr} [%]	i_{corr} [µA/cm²]	Error i_{corr} [%]	CPR [mmpy]	Error CPR [%]
SS (a)	-0.382	4.9	297.02	14.6	3.050	14.6
(b)	-0.325	3.5	6.963	5.8	0.072	5.8
(c)	-0.330	11.4	6.374	17.1	0.065	17.1
[10]	(-0.365)		(400)		(4.3)	
Ni TF	-0.127	20.3	1.695	34.9	0.018	34.9
[11]	(-0.121)		(0.55)		(0.006)	
S235	-0.546	0.5	253.1	8.6	2.97	8.6
[12]	(-0.607)		261.9		(3.07)	

a) *Stainless steel 1.4301*

Comparison of the corrosion potential determined for the stainless steel samples turned of a rod with the one reported in literature reveals a good agreement with only minor difference of 0.017 V. The corrosion rate calculated for the studies presented in this application note is approximately 30 % lower than the literature value, thus also showing sufficient agreement taking into account the diverging results normally expected in corrosion studies, so that corrosion rates diverging by a factor of two to three are regarded as equal [2].

Regarding the differently pretreated stainless steel 1.4301 specimen laser cut from a rolled stainless steel sheet, there is only a negligible difference in corrosion potential of 0.005 V between polished and by abrasive paper treated ones. For the latter samples the corrosion current and thus the rate was less than 10 % lower than for the polished one, thus also showing good agreement. With respect to the diverging results normally expected in corrosion studies, the difference observed for the two different surface treatments should be within this error and thus insignificant [2].

[14] J. M. Esteban, M. E. Orazem, ***J. Electrochem. Soc.*** **138**, 1, (1991), 67-76

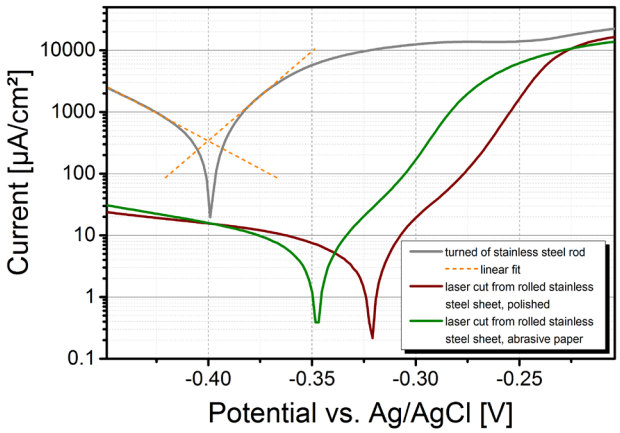

Figure 3: Representative plot of the polarization curves of the three differently treated stainless steel 1.4301 specimen used for determination of E_{corr} and i_{corr} by Tafel analysis. For sake of clarity the linear fits are only shown exemplarily for the specimen turned of a stainless steel rod, but were likewise performed for all other samples analysed using Tafel analysis and displayed as dashed lines. Scan speed and temperature during measurement were 1.66 mV/s and 20.0 °C, respectively. The respective stainless steel specimen were used as working electrode, while platinum and 2 mol/l HCl were employed as counter electrode and electrolyte, respectively.

In contrast, the set of samples turned of a stainless steel rod showed distinctly higher corrosion rate being more than 42 times higher in comparison to the rolled metal sheets and the corrosion potential is shifted to more negative potentials. In literature, both beneficial and detrimental effects of rolling are reported [15], [16]. Positive effects of cold rolling resulting in reduced corrosion rates are caused by e.g. hardening, tailoring the microstructures or a higher Cr:Fe ratio in the passive surface film [15], [16], [17].

The shift of the corrosion potential to more noble potentials as well as a reduced corrosion current density for rolled stainless steel specimen in comparison to untreated ones was reported by Phandis et al. comparing rolled and annealed 1.4301 stainless steel in 3.5 % NaCl solution [17]. Annealing of stainless steel specimen after rolling is expected to revoke the positive effect of rolling [16].

Warzee et al. also emphasized the great impact of initial surface treatment of stainless steel on the corrosion rate and revealed cold-work, i.e. rolling, polishing or grinding, as essential factor for lowering of the corrosion rate, while definition of the surface state in terms of its roughness is inadequate [6]. However, during this study the beneficial effect of cold-work was only observed in superheated steam at temperatures higher than 350 °C, but not at lower temperatures or in water. Due to the rather different conditions used in this study in comparison to the ones applied in this application note comparability is rather questionable and they only can be seen as hint reinforcing our results of (a) the lower corrosion rate of the rolled stainless steel specimen in comparison to the untreated ones and (b) the corrosion rate being independent of the different surface roughness achieved by either polishing or usage of abrasive paper.

b) *Nickel thin films*

The results reported in Table 3 for the nickel thin films are the mean values of thin films deposited at 3 V and 2 V, resulting in current densities during thin film preparation of approximately 0.32 A/cm² and 0.07 A/cm², respectively. For each different fabrication two specimen were examined. In accordance with literature the corrosion potential of the thin films deposited at higher current density is slightly lower than for the ones prepared at lower one. However, the mean difference of E_{corr} is only 0.011 V, thus natural fluctuation during corrosion studies also could not excluded as basic cause. More detailed investigations with specimen prepared at more than two diverse current densities would be required for a more reliable statement, which is beyond the scope of this application note. The range of E_{corr} reported in literature for the nickel thin films deposited using diverse current densities ranging from 0.01 to 0.10 mA/cm² is -0.121 to -0.213 V. The value determined during the experiments presented in this application note

[15] L. Peguet et al., ***Corrosion Science* 49** (2007) 1933–1948
[16] C. Garcìa et al., ***Corrosion Science* 43** (2001) 1519–1539
[17] S.V. Phadnis et al., ***Corrosion Science* 45** (2003) 2467–2483

fits with -0.127 V in this range. However, as in the literature source the corrosion potential decreases with increasing deposition current density, a lower value would be expected during our studies. Nevertheless, as not only the deposition current density, but also the total film thickness might influence the corrosion behaviour, a more detailed comparison is not possible based on the published data and beyond the scope of this application note.

Corrosion current and thus the corrosion rate determined during measurements for this application note are approximately three times the mean of the values reported in literature. However, taking into account the different deposition conditions during thin film preparation together with the natural fluctuation of corrosion rates, the accordance is still sufficient [2].

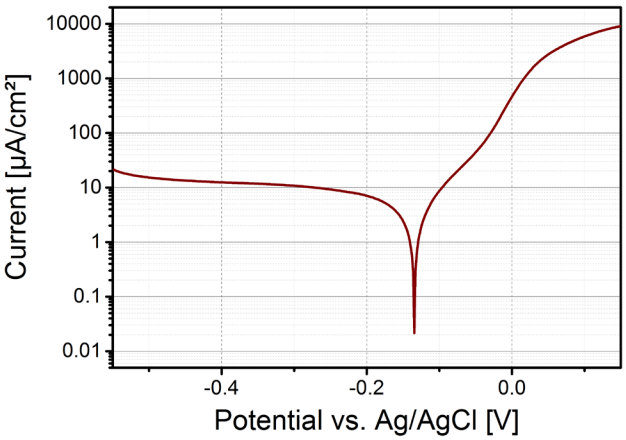

Figure 4: Representative plot of the polarization curve of nickel thin films used for determination of E_{corr} and i_{corr} by Tafel analysis. Scan speed and temperature during measurement were 1.00 mV/s and 25.0 °C, respectively. The nickel thin film was used as working electrode, while platinum and 0.5 mol/l Na_2SO_4 (pH ~ 2) were employed as counter electrode and electrolyte, respectively.

c) *Steel S235*

E_{corr} determined for the S235 steel specimen during measurements made for this application note is approximately 0.06 V higher than reported in literature. However, as only one literature source could be found, its reliability unfortunately could not be proved and a difference of only 0.06 mV nevertheless shows good accordance. Comparison of the corrosion rate shows very good agreement which also should hold for the corrosion current. However, in literature a value half of that calculated from our data is reported, which obviously does not fit to the reported corrosion rate. Inspection of the plots used for Tafel analysis in the literature source also point to higher corrosion currents. It thus stands to reason that erroneous i_{corr} were presented in the literature source, while for calculation of the corrosion rate correct ones were used. Thus, in Table 3 the corrected value recalculated from the corrosion rate given in the literature source is represented.

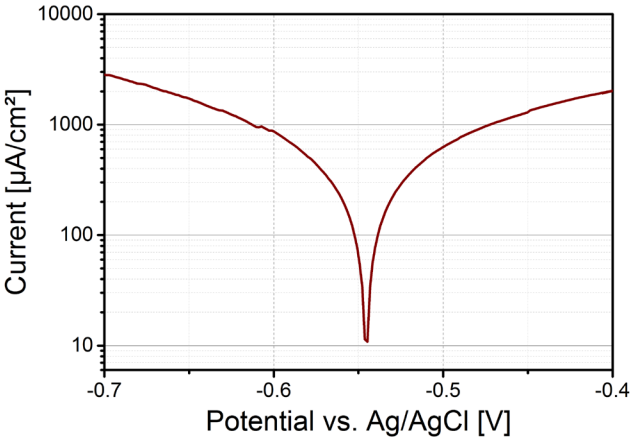

Figure 5: Representative plot of the polarization curve of steel S235 used for determination of E_{corr} and i_{corr} by Tafel analysis. Scan speed and temperature during measurement were 0.50 mV/s and 25.0 °C, respectively. The steel specimen were used as working electrode, while platinum and 0.5 mol/l HCl were employed as counter electrode and electrolyte, respectively.

Comparison between results achieved using different corrosion test methods exemplarily shown at nickel thin film specimen

a) *Impedance spectroscopy*

In Figure 6 an exemplary impedance spectrum recorded for a nickel thin film sample is shown. The equivalent circuit also presented in this figure was used for fitting of the data for determination of the polarization resistance from impedance spectroscopy. Thereby, *L* symbols an inductor and represents the parasitic inductive artefacts at high frequencies

due to e.g. connection cables. R_b is an ohmic resistor and typifies the resistance of the cables as well as the resistance due to bulk ion transport. R_p is the polarization resistance. The constant phase element CPE takes interface effects, i.e. charging of the electrochemical double layer at the interface electrode/sample, into account.

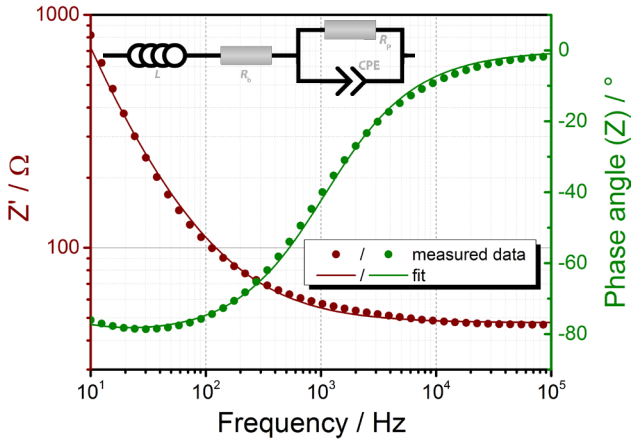

Figure 6: Exemplary Bode plot of the impedance measurement of a nickel thin film sample plotting on the left and right ordinate the real part of the impedance Z' and the phase angle, respectively, together with the equivalent circuit representing the impedance behaviour of the samples within the chosen frequency range.

b) *Polarization resistance technique*

For determination of the polarization resistance via polarization resistance technique the data recorded for Tafel extrapolation were also used, although strictly spoken in this evaluation technique only a small potential range around E_{corr} is measured. For determination of R_p the measured current density was plotted linearly vs. the applied potential, see exemplarily Figure 7, and slope of the data in the vicinity of the corrosion potential was determined using linear extrapolation, thus delivering the reciprocal of R_p. Corrosion current was calculated from this using either Equation 12 solved for i_{corr}:

$$i_{corr} = \frac{RT}{nF} \cdot \frac{\mathrm{d}i}{\mathrm{d}\eta_{CT}} = \frac{RT}{nFR_p} \qquad \textbf{(Equation 16)}$$

or Equation 12.3. Exemplary results are presented for the nickel thin films in Table 4 comparing the corrosion current density and corrosion rate as well as the respective errors determined using Tafel extrapolation, impedance spectroscopy and polarization resistance technique. For the latter two techniques results calculated either using Equation 16, i.e. calculation based on universal constants without usage of Tafel slopes, or Equation 12.3, employing the Tafel slopes determined during Tafel extrapolation, were given.

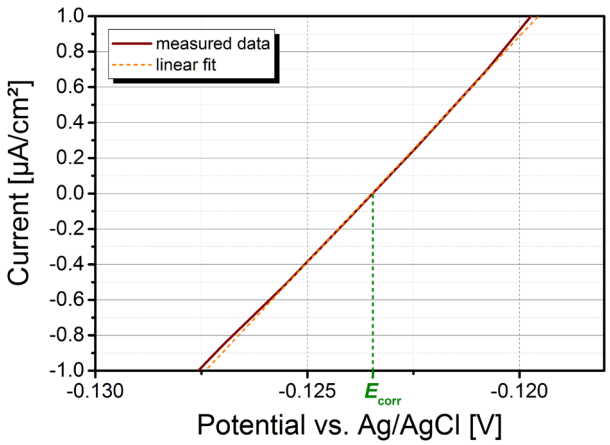

Figure 7: Representative plot of the polarization curve of nickel thin films showing the linear range close to E_{corr} used for determination of i_{corr} by polarization resistance technique together with the linear fit displayed as dashed line. Scan speed and temperature during measurement were 1.00 mV/s and 25.0 °C, respectively. The nickel thin film was used as working electrode, while platinum and 0.5 mol/l Na_2SO_4 (pH ~ 2) were employed as counter electrode and electrolyte, respectively.

Values of the corrosion current density and thus of the corrosion rate determined using polarization resistance technique are slightly higher than by application of Tafel extrapolation. This finding was also reported in literature [18]. In contrast, those determined using impedance spectroscopy are slightly lower. However, the agreement between all three techniques is absolutely sufficient.

Calculation of i_{corr} using either Equation 12.3 or Equation 16, i.e. with or without usage of Tafel slopes, respectively, delivers for both the polarization resistance technique and impedance spectroscopy comparable values. For both techniques usage of Tafel slopes results in slightly higher values and errors. This thus indicates that Tafel slopes are at least for

[18] R. Mishra et al., ***Corrosion Science*** **46** (2004) 3019–3026

the nickel thin film electrodes presented in this application note not necessarily needed for calculation of the corrosion current density from polarization resistance values either determined from polarization resistance technique or impedance spectroscopy, but reliable values can also be achieved using Equation 16 employing universal constants. However, care has to be taken by usage of Equation 16 as during its derivation the assumption was made that both transfer coefficients $\alpha_{a,m}$ and $\alpha_{c,X}$ are equal. This seems to be suitable for the nickel thin film electrodes presented in this application note as usage of Equation 16 delivers values of i_{corr} comparable to the other two techniques applied. However, in case of systems with unknown transfer coefficients calculation of i_{corr} should not be solely based on Equation 16 as diverging transfer coefficients for metal oxidation and/or reduction of the species to be reduced could result in distinct errors.

Table 4: Comparison of the corrosion current density and corrosion rate as well as the respective errors determined using different electrochemical analysis methods for the nickel thin films. Errors are given as maximal deviation from the mean. Method (a) uses Equation 16 for calculation, i.e. calculation based on universal constants without usage of Tafel slopes, while (b) uses Equation 12.3 employing the Tafel slopes determined during Tafel extrapolation.

Analysis method	i_{corr} [µA/cm²]	Error i_{corr} [%]	CPR [mmpy]	Error CPR [%]
Tafel extrapolation	1.695	34.9	0.018	34.9
Polarization resistance technique				
(a)	2.647	23.6	0.029	23.6
(b)	3.13	30.6	0.034	30.6
Impedance spectroscopy				
(a)	0.987	13.6	0.011	13.6
(b)	1.180	44.9	0.013	44.9

The good agreement of all three different techniques used for determination of i_{corr} leads to the conclusion that at least for the metal specimen investigated during this study Tafel extrapolation technique going along with longer measurement times and the major drawback that due to surface changes during potential scan covering a large range with distinct deviations from the corrosion potential requiring repreparing of the samples after every measurement is not needed, but faster techniques like polarization resistance technique or impedance spectroscopy enabling the repeated measurement of one single sample also deliver reliable results.